Mat. Res. Soc. Symp. Proc. Vol. 692 © 2002 Materials Research Society

Deep Centers and Their Capture Barriers in MOCVD-Grown GaN

Daniel K. Johnstone[a], Mohamed Ahoujja[b], Yung Kee Yeo[c], Robert L. Hengehold[c], Louis Guido[d]
[a]Air Force Office of Scientific Research, Arlington, VA 22203, USA
[b]University of Dayton, Dayton, OH 45469, USA
[c]Air Force Institute of Technology, Wright-Patterson AFB, OH 45433, USA
[d]Virginia Polytechnic Institute and State University, Blacksburg, VA 24061, USA

ABSTRACT

GaN and its related alloys are being widely developed for blue-ultraviolet emitting and detection devices as well as high temperature, high power, and high frequency electronics. Despite the fast improvement in the growth of good quality GaN, a high concentration of deep level defects of yet unconfirmed origins are still found in GaN. For both optical and electronic devices, these deep carrier traps and/or recombination centers are very important and must therefore be understood. In the present work, deep level defects in GaN grown on sapphire substrates by metal organic chemical vapor deposition (MOCVD) have been investigated using Isothermal Capacitance Transient Spectroscopy (ICTS) and Current Voltage Temperature (IVT) measurements. Several deep level electron traps were characterized, obtaining the emission energy, concentration, and capture cross section from a fit of exponentials to the capacitance transients. ICTS was also used to reveal information about the capture kinetics involved in the traps found in GaN by measuring the amplitude of the capacitance transient at each temperature. At a reduced filling pulse where the traps were not saturated, several of them showed marked reduction in capacitance transient amplitude when compared to the transient amplitude measured under conditions where the filling pulse saturates the traps. This reduction in transient amplitude indicates that there is a barrier to carrier capture, in addition to the emission barrier. It has been found that several traps had capture barriers that were significant fractions of the emission energies up to 0.32 eV. These capture barriers may lead to persistent photoconductivity and reduced trapping. In this paper, deep level emission energies as well as capture barrier energies found in MOCVD-grown GAN will be discussed.

INTRODUCTION

In spite of considerable work to develop gallium nitride based materials, there is still much to be done to understand the nature of the defects. GaN is desirable for applications toward higher density memory,[1] high power microwave devices and high temperature devices,[2-4] and UV photodetection.[5-7] Current studies of the material include investigations of dopants to increase the carrier activation,[8] metallizations to reduce contact resistance or improve rectifying ideality,[9-11] extensive efforts to improve the quality of the epitaxial material, and myriad characterization methods that have been employed to understand the origin and role of defects.[12-14] Lack of high quality lattice-matched substrates for epitaxy is receiving most of the development focus. Epitaxial growth on sapphire and silicon carbide are two of the more prevalent methods. Silicon substrates are also being used. Growth is accomplished by many of the common methods including molecular beam epitaxy, metal-organic chemical vapor deposition (MOCVD), vapor phase epitaxy, and others. Circumventing the high density of threading dislocations has lead to innovative approaches such as lateral epitaxial overgrowth,[15,16] and pendeo-epitaxy,[17,18] but also using thick buffer layers.[19,20] The success of these efforts has

been progressing steadily, interspersed occasionally with devices that have demonstrated record performance. However, much of the work has demonstrated the limited maturity of the material, compared to other zincblende III-Vs. Current collapse in field effect devices is one of the difficulties that are presently being addressed.[21, 22] Limited lifetime for lasers based on nitrides also presents a vexing problem.[23] High concentrations and varied types of defects are recognized as the source of these difficulties. Understanding the characteristics of these defects is an important step in reducing their effects.

EXPERIMENTAL

ICTS diode preparation

GaN films were grown using MOCVD technique using a standard two-step growth process, beginning with a 300 Å GaN buffer layer grown at 550 °C on sapphire substrates, followed by a 2 μm thick n-type GaN test layer. Before contact fabrication, the samples were degreased in solvents, followed by an acid clean in aqua regia (HCl:nitric acid = 3:1) and a dip in de-ionized water. Ohmic contacts were made by depositing Ti(400 Å)/Al(2000 Å), and alloying them under an N_2 atmosphere at 900 °C for 30 seconds in a rapid thermal anneal system. Schottky barrier diodes were made by using a 250 μm diameter of Ni(1000 Å)/Au(1000 Å) contacts. Room temperature carrier concentration is ~$8x10^{16}$ cm^{-3}, while the room temperature mobility is 250 $cm^2/V \cdot sec$.

Deep level characterization

Deep levels in epitaxial GaN were characterized using isothermal capacitance transient spectroscopy (ICTS) and by current-voltage-temperature (IVT) measurements. The ICTS experimental setup uses a data acquisition board to record the entire capacitance transient, and fits the recorded transients for one or two exponential components. The capacitance is measured using a SULA meter with minimum conversion time of 10 μsec. Data acquisition is performed by a high-resolution 16-bit National Instruments board. Representative conditions are to record ~400 points, averaged over ~1000 transients at each temperature, stepping the temperature every 2-5 K. The ICTS equipment can detect a deep level concentration of ~$5x10^{-5}$ n_s and greater, where n_s is the shallow carrier concentration. Once the transients are acquired, they are fit using modulating functions and least squares analysis[24] or commercial curve fitting software. This method of exponential transient fitting has the capability of separating several overlapping emission signals. The analysis fits the capacitance as a function of time, t, given by

$$C(t)^2 = \sum_{i=0} A_i \exp(-e_i t), \qquad (1)$$

where A_i is the squared amplitude of the transient due to the i^{th} energy level at a given temperature. A_0 is the steady state value of capacitance squared with e_0=0, and e_i is the emission rate of the i^{th} energy level. The transients can be fit for one, two, or three exponential components. Then the emission rates are taken from the fit with the smallest least squares error and used to form the Arrhenius plot. The activation energy of the trap is obtained from the slope of the Arrhenius plot, and the capture cross section is obtained from the vertical axis intercept. The trap concentration is determined from the amplitude of each transient. The method of recording and fitting the entire transient used here has been shown to be more accurate than rate-

window methods.[25] As data acquisition has become faster and available as an add-in board for personal computers, the method of recording and analyzing the entire transient is gradually replacing the earlier method of rate windows.

Typically, the trap energy, capture cross section, and concentration are reported characteristics. Analysis assumes that the measured characteristics of the capture cross section are not dependent on temperature. This condition is met if the filling pulse is long enough to saturate the traps over the temperature range of interest. However, several models of capture have been proposed, some of which are temperature dependent. More thorough investigation of the capture cross sections of traps will contribute to the better understanding of the materials, and contribute to the understanding of each of the models. Recording the entire transient capacitance versus time and temperature facilitates measurement of the capture barrier using a single temperature scan. Otherwise, several temperature scans must be done using the rate window method, varying the filling pulse width each time.[26] Adding the capture mechanisms to the other deep level characteristics that are usually reported will provide more accurate information for predicting carrier lifetimes used in device design.

Among the models for capture, three of the more prominent capture processes are cascade capture, capture by multi-phonon emission, and capture associated with Auger recombination. Lax proposed the model of capture as an electron cascading through closely spaced, extended states.[27] The carrier loses energy by emitting a phonon between each extended state. The process of cascade capture has negative temperature dependence as an exponent of temperature, T^{x}. A deeper Coulombic level would have lower energy levels spaced too far apart to allow transitions accompanied by the loss of only one phonon. In this case, simultaneous emission of multiple phonons has been shown to take place.[28] As opposed to cascade capture, multi-phonon emission has a cross section that increases exponentially with increasing temperature, with a characteristic activation energy. The energy loss can be realized by a relaxation or a distortion of the lattice. The method used in this paper to extract the activation energy applies only to capture barriers due to multi-phonon emission.

In an ICTS experiment, a filling pulse that saturates the trap is required in order to obtain accurate trap emission energy and capture cross section from the Arrhenius plot. If saturating conditions are achieved, then the trap depth, E_T, and the capture cross section, σ, are obtained from the slope and intercept of a plot of the emission rate versus $1/kT$, respectively. Alternatively, the capture barrier can be measured by using a narrower, non-saturating filling pulse. The barrier for capture by multi-phonon emission is evident from the change in the amplitude of the capacitance transient as the temperature increases.

The concentration of filled traps, N_T^0, is

$$N_T^0 = N_T\left[1-\exp\left(-t_f \sigma_\infty v_{th} n_s e^{-\frac{E_b}{kT}}\right)\right]. \qquad (2)$$

N_T is the total trap concentration, t_f is the filling pulse width, σ_∞ is the high temperature capture cross section, v_{th} is the thermal velocity, n_s is the shallow carrier concentration. E_b is the activation energy of the capture process, k is Boltzmann's constant, and T is the temperature. In practice, to measure the capture barrier, the temperature is set for maximum response from the trap. Then the pulse width is reduced until there is a reduction in capacitance transient amplitude, but wide enough so that the transient amplitude is well above the noise level. Next, the transients are recorded at temperature steps covering the entire temperature range where the trap responds. Equation (2) shows that as the temperature increases, the concentration of filled

traps increases until the exponential term goes to zero and the trap is saturated. The change in concentration of filled traps is reflected in the amplitude of the capacitance transient.

Fitting of the capacitance transients provides trap concentration versus temperature, which can then be fit according to equation (2) to obtain the capture barrier energy. This method is similar to other methods of measuring the capture barrier but doesn't require the complexities of repeated temperature scans or elaborate pulse shaping.[29,30]

Equation (2) can be reorganized to facilitate extraction of the capture barrier energy using the familiar Arrhenius relationship, as in the analysis by Criado, et al.:[29]

$$\ln(1 - C/C_0) = KT^{\frac{1}{2}} \exp(-E_b/kT). \quad (3)$$

C is the capacitance transient amplitude at temperature T using a filling pulse of width t_f, C_0 is the transient capacitance amplitude for a very long charging time, K is a proportionality factor that is constant with temperature. This equation is appropriate if capture is by multi-phonon emission.

RESULTS

Figure 1a shows the ICTS spectra for the n-type GaN grown by MOCVD under two different filling pulse conditions. The filling pulse width was 10 msec and 50 μsec for these rate window plots. Curve fitting analysis of the three peaks reveals four traps. The corresponding Arrhenius plot is shown in figure 1b. The characteristics of E1 and E2 are E_T=0.190 eV, σ=3x10^{-15} cm^2, and E_T=0.253 eV, σ=9x10^{-16} cm^2, respectively. The peak at 300K was deconvolved to two traps labeled E3 and E4, with characteristics E_T=0.548 eV, σ=2x10^{-15} cm^2, and E_T=0.613 eV, σ=9x10^{-15} cm^2, respectively.

The result of the IVT measurements are shown in figure 2. The energy levels are measured for three values of the reverse bias, -1 V, -2 V, and -3 V. The dominant generation center from IVT measurements is at 0.54 eV. As the reverse bias increases, the measured energy decreases, as shown in the figure. The reduction in generation center energy with increasing reverse bias reveals the donor nature of this deep level.

Reducing the filling pulse from 10 msec down to 50 μsec was used to detect traps with a temperature dependent capture cross section. The traps at E2, E3 and E4 all showed evidence of a temperature dependent capture cross section. Further measurements were made for analyzing the transient amplitude as a function of temperature, in order to obtain more information regarding the trapping mechanism.

Further evidence is shown in plots of the concentration of filled traps as a function of temperature, which are obtained from the amplitude of the transients as they change with temperature. The amplitude obtained for the low temperature peaks is plotted in figure 3a with and without the saturating filling pulse for the traps appearing in the rate window plot between 100K and 175K. Note that trap E1 has a higher concentration with a reduced filling pulse width, although it is not evident from the rate window plot of figure 1. Trap E2 shows the behavior that is expected for reduced filling pulse width, where the curves merge at sufficiently high temperature.

The amplitude data extracted from the capacitance transients between 275K and 400K are shown in figure 3b. An interesting observation is that the two traps show competing trapping behavior. Trap E3 is filled at the expense of trap E4 over a broad range of temperature from 300 to 340K. This behavior can be explained as arising from a defect that can trap two electrons. The emission energy for the second trapped electron is reduced due to Coulomb repulsion.

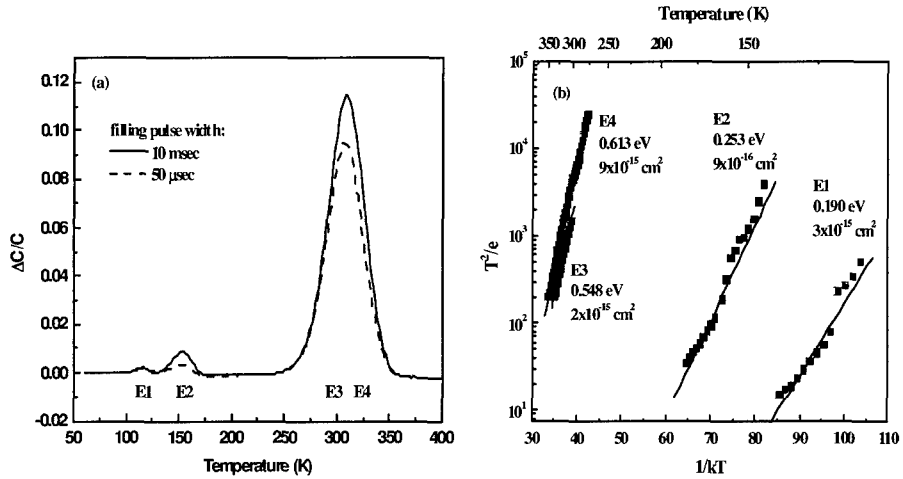

Figure 1. **a.** Rate-window plot for n-type GaN grown by MOCVD. The rate window is 51/sec. **b.** Arrhenius plots for n-GaN grown by MOCVD for each peak in figure 1a.

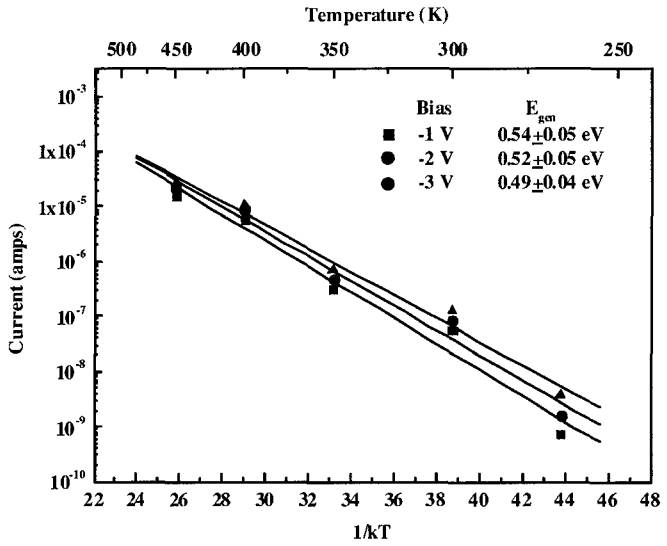

Figure 2. Arrhenius plot from the IVT measurements. The generation current activation energy decreases with increasing reverse bias.

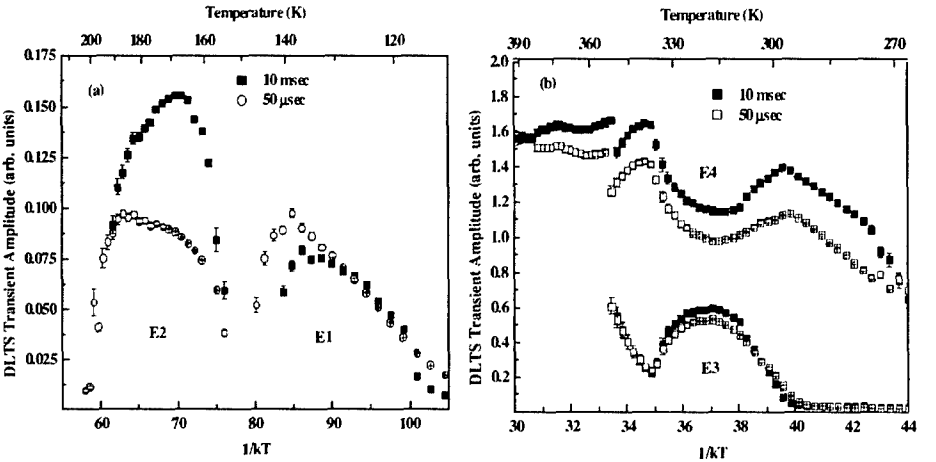

Figure 3. **a)** Comparison of the transient amplitude (concentration) of filled traps from a saturating 10 msec filling pulse and a non-saturating 50 μsec filling pulse for MOCVD grown GaN for the pair of peaks shown at low temperature in figure 1a. **b)** Capacitance transient amplitude for GaN grown by MOCVD. The data corresponds to the peak near room temperature in the rate window plots of figure 1a. The lower curves correspond to the 0.548 eV trap and the upper curves correspond to the 0.613 eV trap.

Capture barriers for the traps were determined using equation 3. Although, the signal strength was not high enough for analysis of the capture barrier for E1 and E2. Figure 4 shows the capture barriers for E3 and E4. The trap E3 at 300K has a capture barrier of 0.32 eV as shown in the figure. Trap E4, with higher concentration, has a capture barrier of 0.12 eV.

DISCUSSION

Trap E1 is very similar to a trap that has been attributed to a nitrogen vacancy.[31,32] If E1 and E2 are part of a defect that can trap two electrons, the reduced filling pulse preferentially fills traps with one electron. A wider filling pulse should fill the defect with two electrons. However, the emission energy of the trap filled with two electrons would be expected to be lower due to Coulomb repulsion. The observation of higher occupation of the lower energy trap, E1, at narrow filling pulse with is evidence for assignment of a negative U binding energy arrangement, where the configuration changes to make the trapping of two electrons more tightly bound than one electron. Trap E2 has been reported previously for several different growth methods, although the origin has not been determined.[33,34]

Other studies of the electron trap E3 at 0.55 eV in various heterostructures found that the density of the trap does not change much from structure to structure or from undoped to Mg doped p-GaN.[35] It is a commonly reported deep level in GaN grown under many different conditions, suggesting that it is not related to impurities.[35,36] The coupled relationship between the traps at 0.55 and 0.61 eV in the present work, labeled E3 and E4, respectively, indicate that

the trap at 0.55 eV is a defect complex with the 0.61 eV trap. Also, Hullavarad *et al.* reported that the 0.6 eV level has its origin in nitrogen vacancies and vacancy clusters.[37]

The IVT measurement of a dominant generation center at 0.54 eV at –1 V corresponds to the trap labeled E4 at 0.61 eV measured with ICTS at –1.5 V. IVT is an equilibrium measurement, where ICTS measurements are made under nonequilibrium conditions. Therefore, IVT will measure the energy difference between the ground state of the defect and the bottom of the conduction band. The energy measured by ICTS is from the ground state of the defect to the top of the capture barrier energy, which is 0.12 eV for E4. The difference between the emission energy and the capture barrier energy measured by ICTS is thus 0.49 eV, which compares well to a value of 0.53±0.05 eV for IVT, when interpolated to –1.5 V. E4 is also expected to be the dominant defect because of its position nearest to mid-gap, larger cross section, smaller capture barrier, and higher concentration compared to the other traps that are present.

The remarkable feature of these measurements is the common occurrence of capture barriers for many of the traps. Several other studies have also observed evidence for capture barriers. In other work, four energy levels were characterized in GaN on sapphire, each of which had thermal ionization energy less than the value of the optical ionization energies.[38] In that study, an increase in photoionization cross section with increasing illumination energy was reported, similar to the studies of the DX center in AlGaAs. The difference in optical and thermal ionization energies and the increase in photoionization cross section are due to a lattice relaxation associated with a capture barrier for the DX center. Polyakov, *et al.* has also pointed out that persistent photoconductivity (PPC), which is due to the presence of a capture barrier, is a common feature in GaN and can be responsible for the current collapse in field effect transistors.[39] A capture barrier of 0.2 eV was measured in their work, although the associated thermal emission energy was unknown. The reason they suggested for the capture barrier was

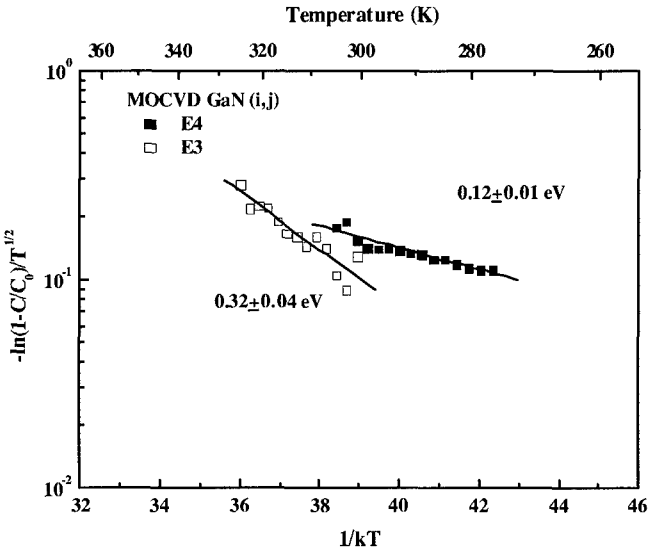

Figure 4. Arrhenius plots for GaN grown by MOCVD. The energies given are the capture barriers for the traps shown in Fig. 5.

that it is due either to a lattice relaxation, or to electrostatic potential variations in the samples resulting from non-uniformly distributed, electrically active donor and acceptor centers.

An alternative explanation for the prevalence of capture barriers could be offered by the very strong piezoelectric effect found in GaN. The lack of inversion symmetry in nitrides gives rise to piezoelectric effects when strained along [0001], which can be an order of magnitude larger than other III-Vs.[40] In addition to the strain effects, the greater screening of defects by surrounding core ion charges, reflected by the larger polarizability in GaN, needs to be taken into account. It is possible that the electrons bound to ions surrounding the defect shift toward or away from the defect to a greater extent than in other III-V materials, such as GaAs, creating a potential barrier. The effect has been addressed in applications toward nitride quantum well structures, but not for point defects or defect complexes.[41]

CONCLUSION

Four electron traps were measured by ICTS in MOCVD GaN. The deep levels are measured at E1=0.190 eV, E2=0.253 eV, E3=0.548 eV, and at E4=0.613 eV. The dominant generation center was determined by IVT to be the donor trap E4. Changes in the filling pulse width showed the presence of capture barriers in several of the traps. Additional analyses were performed to extract the amplitude of the capacitance transients as a function of temperature, both for saturating filling conditions and non-saturating filling conditions, in order to obtain the capture barriers. E1 and showed a behavior consistent with a defect center having a negative U binding energy arrangement. Displaying the transient amplitude as a function of temperature also revealed coupled defect behavior between E3 and E4 where E3 was filled at the expense of the occupation of E4. Capture barriers were determined to be 0.32 eV for E3, and 0.12 eV for E4. The prevalence of capture barriers is suggested to be a basic property of the nitrides, which may be due to the large polarizability, requiring further study.

REFERENCES

1. A. Hayami, M. Mochizuki, J. Tonami, H. Nakamura, and M. Itonaga, "High density optical disk system using D8-15 modulation code and new signal-processing techniques," *IEEE Transactions on Consumer Electronics* **46**, pp. 555-561, 2000.
2. L. Zhang, L. Lester, A. Baca, R. Shul, P. Chang, C. Willison, U. Mishra, S. Denbaars, J. Zolper, "Epitaxially-grown GaN junction field effect transistors," *IEEE Transactions on Electron Devices* **47**, pp. 507-511, 2000.
3. K. Kunihiro, K. Kasahara, Y. Takahashi, Y. Ohno, "Microwave performance of 0.3-μm gate-length multi-finger AlGaN/GaN heterojunction FETs with minimized current collapse," *Jpn. J. Appl. Phys. Suppl.* **39**, pp. 2431-2434, 2000.
4. S. Binari, W. Kruppa, H. Dietrich, G. Kelner, A. Wickenden, J. Freitas, "Fabrication and characterization of GaN FETs," *Solid-State Electron.* **41**, pp. 1549-1554, 1997.
5. A. Saxler, "A review of the electrical properties of $Al_xGa_{1-x}N$ materials for UV photodetector applications," *Proceedings of the SPIE* **3948**, pp. 330-341, 2000.
6. P. Sandvik, D. Walker, P. Kung, K. Mi, F. Shahedipour, v. Kumar, X. Zhang, J. Diaz, C. Jelen, M. Razeghi, "Solar-blind $Al_xGa_{1-x}N$ p-i-n photodetectors grown on LEO and non-LEO GaN," *Proceedings of the SPIE* **3948**, pp. 265-272, 2000.

7 . C. Pernot, A. Hirano, M. Iwaya, T. Detchprohm, H. Amano, I. Akasaki, "Solar-blind UV photodetectors based on GaN/AlGaN p-i-n photodiodes," *Jpn. J. Appl. Phys., Pt.2* **39**, pp. L387-389, 2000.
8 . K. Kim, C. Oh, W. Lee, K. Lee, G. Yang, C. Hong, E. Suh, K. Lim, H. Lee, D. Byun, "Comparative analysis of characteristics of Si, Mg, and undoped GaN," *Journal of Crystal Growth* **210**, pp. 505-510, 2000.
9 . A. Zeitouny, M. Eizenberg, S. Pearton, F. Ren, "W and W/WSi/$In_{1-x}Al_xN$ ohmic contacts to n-type GaN," *Materials Science and Engineering* **B59**, pp. 358-361, 1999.
10 . J. Rennie, M. Onomura, S. Nunoue, G. Hatakoshi, H. Sugawara, M. Ishikawa, "Effect of metal type on the contacts to n-type and p-type GaN," *Journal of Crystal Growth* **189/190**, pp. 711-715, 1998.
11 . Y. Koyama, T. Hashizume, H. Hasegawa, "Formation processes and properties of Schottky and ohmic contacts on n-type GaN for field effect transistor applications," *Solid-State Electronics* **43**, pp. 1483-1488, 1999.
12 . M. Johnson, S. Fujita, W. Rowland, K. Bowers, W. Hughes, Y. He, N. El Masry, J. Cook, J. Schetzina, J. Ren, J. Edmond, "MBE growth and properties of GaN on GaN/SiC substrates," *Solid-State Electronics* **41**, pp. 213-218, 1997.
13. J. Chaudhuri, M. Ng, D. Koleske, A. Wickenden, R. Henry, "High resolution X-ray diffraction and X-ray topography study of GaN on sapphire," *Materials Science and Engineering* **B64**, pp. 99-106, 1999.
14 . M. Topf, F. Cavas, B. Meyer, B. Kempf, A. Krtschil, H. Witte, P. Veit, J. Christen, "GaN/SiC heterojunctions grown by LP-CVD," *Solid-State Electronics* **44**, pp. 271-275, 2000.
15 . M. Razeghi, P. Kung, P. Sandvik, K. Mi, X. Zhang, V. Dravid, J. Freitas, A. Saxler, "LEO of III-nitride on Al_2O_3 and Si substrates," *Proceedings of the SPIE* **3948**, pp. 320-329, 2000.
16 . Y. Song, S. Choi, J. Choi, J. Yang, G. Yang, "Lateral epitaxial overgrowth of GaN and its crystallographic tilt depending on the growth condition," *Phys. Status Solidi A* **180**, pp. 247-250, 2000.
17 . R. Davis, O. Nam, T. Zheleva, T. Gehrke, K. Linthicum, P. Rajogopal, "Lateral- and pendeo-epitaxial growth and defect reduction in GaN thin films," *Mater. Sci. Forum* **338-342**, pp. 1471-1476, 2000.
18 . T. Zheleva, S. Smith. D. Thomson, K. Linthicum, P. Rajogopal, R. Davis, " Pendeo-epitaxy: a new approach for lateral growth of gallium nitride films," *J. Electron. Mater.* **28**, pp. L5-8, 1999.
19 . E. Koh, Y. Ju Park, E. Kyu Kim, C. Park, S. Hun Lee, J. Hee Lee, S. Ho Choh, "The effect of N^+-implanted Si(111) substrate and buffer layer on GaN films," *J. Cryst. Growth* **218**, pp. 214-220, 2000.
20 . S. Zamir, B. Meyler, E. Zolotoyabko, J. Salzman, "The effect of AlN buffer layer on GaN grown on (111)-oriented Si substrates by MOCVD," *J. Cryst. Growth* **218**, pp. 181-190, 2000.
21. P. Klein, J. Freitas, S. Binari, " Photoionization spectra of traps responsible for current collapse in GaN MESFETs," *Wide-Bandgap Semiconductors for High-Power, High-Frequency and High-Temperature Applications*, pp. 547-552, 1999.
22. P. Klein, J. Freitas, S. Binari, A. Wickenden, "Observation of deep traps responsible for current collapse in GaN metal-semiconductor field-effect transistors," *Appl. Phys. Lett.* **75**, pp. 4016-4018, 1999.

23. G. Hasnain, T. Takeuchi, R. Schneider, S. Song, R. Twist, M. Blomqvist, C. Kocot, and C. Flory, "On-wafer continuous-wave operation of InGaN/GaN violet laser diodes," *Electronic Letters* **36**, pp. 1779-1780, 2000.
24. P. Kirchner, W. Schaff, G. Maracas, L. Eastman, T. Chappell, C. Ransom, "The analysis of exponential and nonexponential transients in deep-level transient spectroscopy," *J. Appl. Phys.* **52**, pp. 6462-6470, 1981.
25. W. Doolittle, A. Rohatgi, "A new figure of merit and methodology for quantitatively determining defect resolution capabilities in deep level transient spectroscopy analysis," *J. Appl. Phys.* **75**, pp. 4570-4575, 1994.
26. D. Lang, "Deep-level transient spectroscopy: a new method to characterize traps in semiconductors," *J. Appl. Phys.* **45**, pp. 3023-3032, 1974.
27. M. Lax, "Cascade capture of electrons in solids," *Phys. Rev.* **119**, pp. 1502-1523, 1960.
28. C. Henry, D. Lang, "Nonradiative capture and recombination by multiphonon emission in GaAs and GaP," *Phys. Rev. B, Solid State* **15**, pp. 989-1016, 1977.
29. J. Criado, A. Gomez, E. Calleja, and E. Munoz, " Novel method to determine capture cross-section activation energies by deep-level transient spectroscopy techniques," *Appl. Phys. Lett.* **52**, pp. 660-661, 1987.
30. A. Palma, J. Jimenez-Tejada, J. Banqueri, P. Cartujo, and J. Carceller, "Accurate determination of majority thermal-capture cross sections of deep impurities in p-n junctions," *J. Appl. Phys.* **74**, pp. 2605-2612, 1993.
31. Z.-Q. Fang, D. Look, W. Kim, Z. Fan, A. Botchkarev, and H. Morkoc, "Deep centers in n-GaN grown by reactive molecular beam epitaxy," *Applied Physics Letters* **72**, pp. 2277-2279, 1998.
32. F. Auret, S. Goodman, G. Myburg, F. Koschnick, J. Spaeth, B. Beaumont, and P. Gilbart, "Defect introduction in epitaxially grown n-GaN during electron beam deposition of Ru schottky contacts," *Physica B* **273-274**, pp. 84-87, 1999.
33. C. Wang, L. Yu, S. Lau, E. Yu, W. Kim, A. Botchkarev, H. Morkoc, " Deep level defects in n-type GaN grown by molecular beam epitaxy," *Applied Physics Letters* **72**, pp. 1211-1213, 1998.
34. P. Hacke, H. Okushi, T. Kuroda, T. Detchprohm, K. Hiramatsu, N. Sawaki, "Characterization of mid-gap states in HVPE and MOVPE-grown n-type GaN," *Journal of Crystal Growth* **189/190**, pp. 541-545, 1998.
35. A. Polyakov, N. Smirnov, A. Govorkov, M. Mil'vidskii, A. Usikov, B. Pushnyi, and W. Lundin, "Deep centers in AlGaN-based light emitting diode structures," *Solid State Electronics* **43**, pp. 1929-1936, 1999.
36. H. Cho, C. Hong, K. Kim, E. Suh, and H. Lee, "Deep levels in GaN grown by metalorganic chemical vapor depositions," *Ungyong Mulli* **12**, pp. 456-461, 1999.
37. S. Hullavarad, S. Bhoraskar, S. Sainkar, S. Badrinarayanan, A. Mandale, V. Ganesan, "Deep levels in GaN grown by nitridation of GaAs (110) surface in a electron cyclotron resonance ammonia plasma," *Vacuum* **55**, pp. 121-126, 1999.
38. T. Kang, S, Yuldashev, C. Park, C. Chi, S. Park, Y. Ryu, and T. Kim, "Deep levels in GaN epilayers grown on sapphire substrates," *Solid State Communications* **112**, pp. 637-642, 1999.
39. A. Polyakov, N. Smirnov, A. Govorkov, M. Shin, M. Skowronski, D. Greve, "Deep centers and their spatial distribution in undoped GaN films grown by organometallic vapor phase epitaxy," *Journal of Applied Physics* **84**, pp. 870-876, 1998.

40. H. Morkoc, R. Cingolani, B. Gil, "Polarization effects in nitride semiconductor device structures and performance of modulation doped field effect transistors," *Solid-State Electronics* **43**, pp. 1753-1771, 1999.
41. H. Jiang and J. Singh, "Gain characteristics of InGaN-GaN quantum wells," *IEEE Journal of Quantum Electronics* **36**, pp. 1058-1064, 2000.